New Fluorescent Calcium Indicators Designed for Cytosolic Retention or Measuring Calcium Near Membranes

Charles Vorndran, Akwasi Minta, and Martin Poenie
Department of Zoology, University of Texas at Austin, Austin, Texas 78712-1064 USA

ABSTRACT A new family of fluorescent calcium indicators has been developed based on a new analog of BAPTA called FF6. This new BAPTA analog serves as a versatile synthetic intermediate for developing Ca^{2+} indicators targeted to specific intracellular environments. Two of these new Ca^{2+} indicators, fura-PE3 and fura-FFP18, are described in this report. Fura-PE3 is a zwitterionic indicator that resists the rapid leakage and compartmentalization seen with fura-2 and other polycarboxylate calcium indicators. In contrast to results obtained with fura-2, cells loaded with PE3 remain brightly loaded and responsive to changes in concentration of cytosolic free calcium for hours. Fura-FFP18 is an amphipathic indicator that to binds to liposomes and to cell membranes. Studies to be detailed later indicate that FFP18 functions as a near-membrane Ca^{2+} indicator and that calcium levels near the plasma membrane rise faster and higher than in the cytosol.

INTRODUCTION

The tetracarboxylate fluorescent calcium indicators such as fura-2, indo-1, and fluo-3 are sensitive and popular tools for monitoring the concentration of cytosolic free calcium ($[Ca^{2+}]_i$) in living cells (Grynkiewicz et al., 1985). However, the widespread use of these indicators has also revealed numerous problems and anomalies pertaining to loading of the acetoxymethyl ester (AM ester), dye leakage, accumulation of dye in organelles, spectral alterations between intracellular dye and that in free solution, and unwanted binding of the indicator to cellular constituents (Almers and Neher, 1985; Di Virgilio et al., 1988; Malgaroli et al., 1987; Goligorsky et al., 1986; Steinberg et al., 1987; Poenie et al., 1986; Poenie, 1990; Hollingsworth and Baylor, 1987).

One of the most common problems seen with fura-2 is its tendency to both leak out of cells and accumulate in organelles (Di Virgilio et al., 1990; Goligorsky et al., 1986). Rates of dye leakage can be so high in some cell types that it becomes difficult to load enough dye into the cytosol for measurements. More commonly, cells initially load evenly, but soon the indicator leaks out of the cytosol with the remaining fluorescence largely associates with organelles. Problems with leakage and compartmentalization are not limited to cells that are loaded using the cell permeant AM ester because cells microinjected with the fura-2 anion show similar problems. These problems can be partly remedied with organic anion transport inhibitors such as probenecid or with an indicator linked to dextran. However, the use of probenecid adds unknown variables to the experiment, and dye-dextran conjugates must be microinjected. It would be desirable, therefore, to develop indicators that do not leak out of cells or compartmentalize yet retain the ability to load as an AM ester.

Another problem with fura-2 concerns the ability to detect calcium gradients or calcium transients that are fast or highly localized. There is increasing evidence for microdomains within the cytoplasm in which $[Ca^{2+}]$ may transiently rise to high levels yet are not seen in the cytosol at large (Hernandez-Cruz et al., 1990; Llinas et al., 1992; Rizzuto et al., 1993). Indeed, there are several reasons that fura-2 may not be the ideal indicator for detecting localized calcium transients. First, fura-2 has a high affinity for calcium, and in many cases the localized changes in calcium are postulated to attain values in the micromolar to millimolar range, well above the levels where fura-2 saturates (Llinas et al., 1992). Second, localized calcium transients imaged by conventional wide-field microscopy will always appear to be dampened because of signals from the surrounding cytoplasm that contaminate the image. Confocal imaging can alleviate this problem to some degree, but indo-1 is the only ratiometric calcium indicator that can be used with current confocal microscopes and it bleaches very rapidly. Third, cytosolic calcium indicators can diffuse and thus have the potential for acting as a shuttle buffer (Speksnijder et al., 1989). A similar situation was seen in the detection of localized calcium transients using fura-2 in cells transfected with mitochondria-targeted aequorin (Rizzuto et al., 1993).

One way to generate indicators that more accurately reflect changes in $[Ca^{2+}]$ in particular microdomains of the cell is to target the indicator to those microdomains. The advantage here is that a larger fraction of the indicator is confined to regions of the cell where these localized transients take place and diffusion of the indicator is restricted. An example of this approach is seen in efforts to develop a near-membrane calcium indicator recently described by Etter et al. (1994a). Unfortunately, because of their weak

Received for publication 16 September 1994 and in final form 8 August 1995.

Address reprint requests to Dr. Martin Poenie, Department of Zoology, 141 Patterson Laboratories, University of Texas at Austin, Austin, TX 78712. Tel.: 512-471-5598; Fax: 512-471-9651; E-mail: poenie@mail.utexas.edu.

The present address of Dr. Minta is TEFLABS, 9503 Capitol View Drive, Austin, TX.

0006-3495/95/11/2112/00 $2.00

signal and difficult physical properties, these indicators were not very useful.

In this report, we describe the synthesis and characterization of two new Ca^{2+} indicators called fura-PE3 (PE3) and fura-FFP18 (FFP18). These two indicators separately address some of the problems with fura-2 and other tetracarboxylate calcium indicators discussed above. PE3 is designed to resist compartmentalization and leakage by virtue of an added positive charge. FFP18 is similar to PE3 but contains a hydrophobic tail that targets the indicator to lipids and cellular membranes. We show that PE3 can be loaded into cells as an acetoxymethyl ester derivative in much the same way as fura-2 but gives more uniform loading. In addition, cells loaded with PE3 remain uniformly loaded for hours, whereas fura-2 quickly accumulates in organelles and leaks out of the cell. We also characterize FFP18 and show that it will bind to anionic liposomes while remaining brightly fluorescent and sensitive to changes in $[Ca^{2+}]$. However, detailed biological characterization of FFP18 will be presented in a separate study showing that FFP18 binds to cellular membranes and reports much larger and faster calcium transients than are seen in parallel experiments using fura-2 (Etter et al., submitted for publication).

MATERIALS AND METHODS

Organic synthesis

Proton NMR spectra were recorded on a Varian EM390 instrument at 90 MHz. Peaks are reported below using the following convention: NMR (solvent, operating frequency), chemical shift (δ) in ppm from tetramethyl silane, multiplicity (s, singlet; d, doublet; dd, doublet of doublets; t, triplet; q, quartet; m, multiplet; br, broad), spin-spin coupling constant if appropriate, and integrated number of protons. In cases where several adjacent peaks are too close for their integrals to be separated, the total integral for the cluster is given. Compounds are designated by Roman numerals, except for the end products of the synthesis, which are named PE3, FFP18, and FF15.

I–III

The fura-2 intermediate I (1.2 g, 2.75 mmol) and commercially obtained 4-nitro-5-hydroxybenzaldehyde (II) (Aldrich, Milwaukee, WI) were dissolved in 9 ml dry dimethyl formamide (DMF) containing 4 g of anhydrous K_2CO_3 and heated at 120°C for 2 h. The mixture was then poured into water and the resulting precipitate was filtered, washed with water, and dried to give III (1.3 g). This was used for subsequent steps without further purification.

V

The phosphorane (IV) was prepared by adding 1.75 g *t*-butyl bromoacetate to a solution containing 2.0 g triphenyl phosphine in benzene (10 ml). The resulting precipitate was collected by filtration and dried under vacuum. Subsequently, a mixture containing 1.4 g of IV, 1.3 g of III, and 5 g of K_2CO_3 in 10 ml dry DMF was heated with stirring at 110°C for 3 h. The resulting dark-brown solution was then extracted with ethyl acetate, washed with brine, evaporated, and dried under vacuum. The resulting gum was purified by silica gel chromatography using ethyl acetate:hexane to give 1.2 g of the semisolid V (80% yield). NMR ($CDCl_3$, 90 MHz) 7.85, d, 1H, J = 7Hz; 7.40, m, 5H, aromatic; 7.20, m, 6H; 6.40, d, J = 7Hz; 5.0, s, 2H; 4.40, s, 4H; 1.50, s, 9H.

VI–VII

Compound V (110 mg, 0.2 mmol) was dissolved in methylene chloride (10 ml) and hydrogenated using 30 mg of 5% Pt/C in a Parr hydrogenator at 50 psi H_2 for 5 h. Afterward, the catalyst was removed by filtration and the solvent was evaporated under vacuum to give a homogeneous yellow solid (VI), which was one spot by thin-layer chromatography (TLC) The product was then dissolved in 1 ml acetonitrile and alkylated with the addition of 0.35 ml methylbromoacetate, 0.5 ml ethyl diisopropylamine, and 30 mg NaI and refluxing overnight. When TLC showed the reaction had gone to completion, the mixture was diluted with ethyl acetate and filtered to removed the solids. The filtrate was then washed with water, dried over $MgSO_4$ and evaporated under vacuum. Trituration of the gummy residue with methanol gave a solid, VII (130 mg, 83%), which was used without further purification. NMR ($CDCl_3$, 90 MHz) 7.35, s, 5H; 6.80, m, 4H; 6.55, m, 2H; 5.00, s, 2H; 4.30, s, 4H; 4.20, s, 8H; 3.65, s, 12H; 2.80, t, 2H; 2.55, t, 2H; 1.50, s, 9H.

VIII

Compound VII (150 mg, 0.2 mol) was formylated using the Vilsmeyer formylation method described previously for fura-2 (Grynkiewicz et al., 1985). The reaction yielded 110 mg (70%) of VIII. NMR, ($CDCl_3$, 90 MHz) 10.33, s, 1H; 7.20, 2 + m, 6H; 6.70, m, 3H; 6.30, s, 1H; 5.10, s, 2H; 4.25, s, 4H; 4.20, s, 4H; 4.15, s, 4H; 3.65, s, 6H; 3.60, s, 6H; 2.80, t, 2H; 2.55, t, 2H; 1.40, s, 9H.

IX

Compound VIII (90 mg, 0.13 mmol) was debenzylated by hydrogenation over 20 mg 10% Pd/C in acetic acid at 50 psi H_2 overnight. This gave a quantitative yield of compound IX. NMR, ($CDCl_3$, 90 MHz) 11.20, s, 1H; 9.60, s, 1H; 6.90, s, 1H; 6.70, m, 3H; 6.10, s, 1H; 4.10–4.30, m, 12H; 3.60, s, 12H; 2.80, t, 2H; 2.50, t, 2H; 1.45, s, 9H.

X

2-Chloromethyl-5-ethoxycarbonyloxazole was synthesized from ethyl oxalyl chloride, chloroacetonitrile (Aldrich), and copper acetoacetonate (Fluka Chemical Co., Ronkonkoma, NY) as described by Grynkiewicz et al. (1985). Compound IX (250 mg, 0.34 mmol), 2-chloromethyl-5-ethoxycarbonyloxazole (100 mg), K_2CO_3 (250 mg), and dry DMF (1 ml) were then stirred together at 110°C for 1.5 h. When TLC showed that the reaction had gone to completion, the mixture was diluted with ethyl acetate, washed three times with water, dried over anhydrous Na_2SO_4, and evaporated to dryness under vacuum. The resulting gummy residue solidified upon storage at 0–4°C overnight and crystallized upon trituration with methanol to give 200 mg of X (67%). NMR, ($CDCl_3$, 90 MHz) 7.90, s, 1H; 7.50, s, 1H; 7.10, m, 2H; 6.80, m, 3H; 6.45, q, 2H; 4.40, s, 4H; 4.30, s, 4H; 4.20, s, 4H; 3.65, s, 6H; 3.60, s, 6H; 2.80, t, 2H; 2.60, t, 2H; 1.50, s + t; 12H.

XI

X (40 mg) was dissolved and stirred overnight in a solution of 20% trifluoroacetic acid in methylene chloride. The solvent was evaporated under high vacuum at room temperature to give a gummy residue (XI), which was reconstituted in freshly distilled methylene chloride and used in subsequent steps without further purification.

XII

A solution of 2.2 g (14 mmol) methyl bromoacetate in 10 ml chloroform was added dropwise with stirring over the course of 1 h to a solution containing 5 g piperazine (58 mmol) dissolved in 30 ml chloroform. The resulting mixture was filtered to remove solids and evaporated to dryness under vacuum. The residue was then reconstituted in chloroform and purified by silica gel chromatography using 10% methanol:chloroform to give 1.5 g of the monosubstituted piperazine (65%). NMR, ($CDCl_3$, 90 MHz), 3.80, s, 3H; 3.30, s, 2H; 3.05, t, 4H; 2.60, t, 4H; 2.00, s, 1H.

XIII

A solution containing 5 g dodecylbromide (20 mmol) dissolved in 10 ml chloroform was added dropwise with stirring over the course of 1 h to a solution containing 10 g piperazine (116 mmol) dissolved in 50 ml chloroform. The resulting mixture was filtered to remove solids and the filtrate evaporated to dryness under vacuum. The residue was reconstituted in chloroform and purified by silica gel chromatography using 10% methanol: chloroform to give 2 g of monosubstituted piperazine (XIII). NMR, ($CDCl_3$, 90 MHz) 1.30–1.75, m, 25H; 2.30, s, 1H; 2.40, t, 4H; 2.90, t, 4H.

FF15

Compound XI (100 mg) was dissolved in 3 ml freshly distilled methylene chloride, and 120 μl of oxalyl chloride was added. The mixture was then stirred for 20 min at 55°C. Afterward the product was dried under vacuum and immediately resuspended in 2 ml of dry methylene chloride. To this solution, 1 ml of methylene chloride containing 200 mg of dodecylamine (Aldrich) was added and the mixture was stirred for 3 h at room temperature. The resulting crude product was dried under vacuum, resuspended in chloroform, and purified by silica gel chromatography using 10% methanol:chloroform to give 40 mg of FF15 as a gum. NMR, ($CdCl_3$, 90 MHz) 7.90, s, 1H; 7.50, s, 1H; 7.15, d, 2H; 6.80, m, 2H; 4.20–4.50, m, 12H; 3.70, s, 4H; 3.65, s, 4H; 1.20–1.50, m, 25H.

Fura-PE3

Compound XI (40 mg) was dissolved in 1.0 μl freshly distilled methylene chloride, and then 45 μl of oxalyl chloride was added. The mixture was stirred for 20 min at 55°C. After completion, the product was dried under vacuum and redissolved in 1 ml freshly distilled methylene chloride. To this mixture was added 0.5 ml methylene chloride containing 100 mg of XII. The resulting mixture was stirred for 2 h at room temperature to give the crude PE3. This was purified by column chromatography over silica gel eluting with 2% methanol:chloroform to give 25 mg of pure product. NMR, ($CDCl_3$, 90 MHz) 7.80, s, 1H; 7.40, s, 1H; 7.15, s, 1H; 7.00, d, 2H; 6.70, m, 2H; 4.50, q, 2H; 4.40, s, 4H; 4.30, s, 4H; 4.10, s, 4H; 3.70, s, 3H; 3.60, s, 6H; 3.55, s, 6H, 3.20, s, 2H; 2.80, m, 2H; 2.50, m, 10H.

Fura-FFP18

Oxalyl chloride (50 μl) was added to a solution containing 50 mg of compound XI dissolved in 1 ml freshly distilled methylene chloride. The mixture was then stirred for 20 min at 55°C. After completion, the product was dried under vacuum and redissolved in 1 ml freshly distilled methylene chloride. To this mixture was added 1 ml fresh methylene chloride containing 120 mg XIII. The resulting mixture was stirred for 3 h at room temperature and then dried under vacuum. The crude product was redissolved in chloroform and purified by silica gel chromatography using 5% methanol chloroform to give 35 mg of pure FFP18 as a gum. NMR ($CDCl_3$, 90 MHz) 7.80, s, 1H; 7.50, s, 1H; 7.10, d, 2H; 6.85, m, 2H; 3.90–4.40, m, 16H; 3.50, m, 2H; 2.30, m, 2H; 1.10–1.50, m, 25H.

PE3 acetoxymethyl ester

Synthesis of the PE3 acetoxymethyl ester required the PE3 free acid as a starting material. This was prepared by hydrolyzing the PE3 methyl ester using 10 equivalents of KOH in a mixture of dioxane/methanol/water. The hydrolysis was monitored using Whatman MKC18F reverse-phase plates developed with 50% methanol:water. Using this procedure, one can resolve the indicator at various stages of de-esterification. After hydrolysis, the solution was acidified with HCl to pH 2.0, which precipitates the PE3 free acid. The resulting precipitate was washed with dH_2O and then dried thoroughly under vacuum in the presence of P_2O_5.

Acetoxymethyl bromide was prepared from methylene diacetate and trimethylsily bromide (Aldrich) as described by Grynkiewicz et al. (1985). The esterification reaction between PE3 free acid and acetoxymethyl bromide was tested using a variety of solvents in an effort to maximize yield and minimize quaternization of the piperazine amino nitrogen. The best results were obtained using freshly dried and distilled CH_2Cl_2 as the solvent and freshly dried and distilled ethyl diisopropyl amine (EDA) as the base. In a typical preparation, 2 mg of PE3 free acid was mixed with 100 μl CH_2Cl_2 followed by 100 μl acetoxymethyl bromide and 100 μl EDA. The formation of the ester was monitored on thin-layer silica gel plates, using 2% methanol in chloroform as the solvent. When complete, the mixture was diluted into ethyl acetate and washed twice with aqueous $NaHCO_3$. The organic layer was then dried over $MgSO_4$ and the solvent was removed under vacuum. The PE3/AM was purified by silica gel column chromatography, using 2% chloroform:methanol as the solvent. The yield was 1.5 mg or 75%.

UV absorbance and fluorescence spectra

UV absorbance spectra were recorded on a Shimadzu UV-265 spectrophotometer at room temperature. Fluorescence spectra were recorded on a Photon Technology International Alphascan Fluorometer. All fluorescence spectra were acquired without employing the rhodamine quantum counter, and the emission spectra are uncorrected because parameters needed to correct the emission spectra were not supplied with this early version of the instrument. The procedure used to obtain quantum yields is modified from that of Grynkiewicz et al. (1985) and relies on the virtually identical spectral characteristics of PE3, FFP18, and fura-2, along with the previously reported quantum yields of fura-2. Here, the concentration of a calcium-saturated solution of PE3 or FFP18 was adjusted to give the same absorbance at 335 nm as a calcium-saturated solution of fura-2. The integral of the emission spectra at 335 nm excitation was then determined for each solution. This procedure was repeated for the free anion of PE3, FFP18, and fura-2, using 364 nm as the absorbance and excitation wavelength. The integrals (I) for the calcium complex or free anion are then used to calculate quantum efficiency as

$$(I_{\text{sample}}/I_{\text{fura-2}})\Phi_{\text{fura-2}}.$$

Determination of calcium dissociation constants

Dissociation constants were determined from sets of fluorescence excitation spectra recorded during the incremental titration of a sample of indicator with Ca^{2+} or Mg^{2+}. Calcium concentrations were set using CaEGTA buffers. Values for the apparent dissociation constant of EGTA at a given pH and temperature were taken from Tsien and Pozzan (1989). Once a complete set of spectra was obtained for a given titration, a Hill plot ($\log_{10}[Ca_{2+}]$ versus $\log_{10}[(F - F_{\text{min}})/(F_{\text{max}} - F)]$ was used to determine the calcium K_d. Here F_{min} and F_{max} are the fluorescence intensities at limiting low and high $[Ca^{2+}]$, and F is the fluorescence intensity for various intermediate $[Ca^{2+}]$. The K_d is equal to the $[Ca^{2+}]$ when $\log_{10}[(F - F_{\text{min}})/(F_{\text{max}} - F)] = 0$.

To prepare these calcium buffers by the method of Moiescu, and Pusch (1975) and Tsien and Pozzan (1989) requires the careful titration of EGTA to an end point with Ca^{2+} by monitoring the change in pH. Addition of

calcium to an unbuffered solution of EGTA causes the release of protons in exchange for calcium. As EGTA approaches calcium saturation, the change in pH per unit calcium decreases essentially to zero. The choice of an end point by the convention of Tsien and Pozzan (1989) is the point where the pH change drops to half its original value. Two methods were used to determine the end point; one was based on pH and the other required the use of a calcium electrode.

A calcium electrode can also be used to determine the saturation point when a concentrated solution of EGTA is titrated with calcium at high pH. To prepare a solution of 0.5 M CaEGTA using the electrode to find the end point, 9.51 g EGTA (Fluka "puriss" grade) and 1.67 g $Ca(OH)_2$ (BDH) were dissolved in 15 ml ddH_2O and adjusted to pH 10 with concentrated KOH. The solution was then diluted to 30 ml and divided into two aliquots of 15 ml each. A calcium selective electrode (Orion 93–20) and reference electrode (Orion 90–01), whose electrode potentials were previously calibrated against a series of calcium standards (Tsien and Rink, 1980), were then used to monitor calcium concentration as one of the 15-ml aliquots was titrated through an end point. For the titration, 1 M $CaCl_2$ (BDH) was added in 25-μmol increments and the electrode potential was recorded. The plot of electrode potential versus $[Ca^{2+}]$ gives an S-shaped curve where maximum change corresponds to the point of saturation. After the initial inflection point was determined, the remainder of the EGTA solution was added. This reduced $[Ca^{2+}]$ to a point where the electrode potential was well below the inflection point. Calcium was then added in 25-μmol aliquots until the electrode potential equaled the original inflection point. Finally, the CaEGTA solution was brought to volume in a 50-ml volumetric flask.

Cell culture

The 322 T lymphoma cell line (Richie et al., 1988) was grown in RPMI (GIBCO BRL) supplemented with 24 mM $NaHCO_3$, 1 mM glutamine, 1 mM sodium pyruvate, 8% heat-inactivated fetal bovine serum (FBS), 100 units/ml penicillin, and 100 μg/ml streptomycin in a humidified, 37°C, 5% CO_2 incubator (Forma).

Bovine papilloma virus cells (BPV; Rasmussen and Means, 1987), an adherent cell line derived from mouse C127 cells, were obtained as a gift from Dr. Anthony Means. Cells were grown in Dulbecce's modified Eagle's medium supplemented with 10% FBS, 100 units/ml penicillin, 100 μg/ml streptomycin, in a humidified incubator (Forma) maintained at 37°C and 5% CO_2. Cells were trypsinized and plated onto sterile round coverslips 24 h preceding use in an experiment.

Cell loading with PE3/AM or fura-2/AM

For these experiments, 322 cells were suspended at a concentration of 1×10^6 cells/ml in 10 mM HEPES-buffered RPMI (pH 6.8) containing 1% FBS and 2 μM PE3/AM and incubated for 1 h at 37°C. For loading with fura-2/AM the procedure was the same except that the cells were loaded at pH 7.1 and incubated with the AM ester for 30 min. After the incubation, cells were washed by gentle centrifugation and then resuspended in HBSS containing 10 mM HEPES (pH 7.2) and 1% FBS.

For loading of BPV cells, cells adhered to coverslips were transferred to dye-loading medium consisting of RPMI supplemented with 1 mM sodium pyruvate, 2 mM L-glutamine, 10 mM HEPES, and 1% FBS, pH 6.8. Either 8 μM fura-2/AM or PE3/AM was then added to the medium and cells were agitated for 30 min (fura-2) or 1 h (PE3) on an orbital shaker set to 75 rpm while the temperature was maintained at 37°C. Subsequently cells were washed into HBSS containing 10 mM HEPES and 2% FBS and agitated for an additional 5 min on the shaker. Finally, the coverslip was washed with fresh HBSS and mounted in a Sykes-Moore chamber, which was then placed in a temperature-regulated holder on the microscope stage.

Evaluation of cell loading and AM ester hydrolysis

The quality of dye loading was evaluated by comparing the limiting 340 nm/380 nm ratios obtained from a sample of fura-2 or PE3 salt to the corresponding values obtained after dye-loaded 322 T-lymphoma cells were lysed with digitonin. Cells were loaded with either fura-2/AM or PE3/AM, washed, and incubated for 10 min at 37°C. Background fluorescence was determined by measuring the signal of an unloaded cell suspension, and these values were subtracted from the raw fluorescence data. The limiting high Ca^{2+} 340 nm/380 nm ratio (R_{max}) was obtained upon cell lysis with digitonin because the HBSS contains sufficient calcium (1.2 mM) to saturate the indicator. Subsequently, 10 mM EGTA and 20 mM Tris base were added to obtain the limiting low Ca^{2+} ratio (R_{min}). The procedure was repeated using samples of pure fura-2 and PE3 potassium salts; the data are shown in Table 3. The results show that for both indicators, R_{max} values after cell lysis were only 90% of that obtained from a sample of the corresponding salt. Thus while hydrolysis appears to be incomplete, cells hydrolyze the fura-2/AM and PE3/AM esters to the same extent.

Preparation of liposomes

Negatively charged liposomes were prepared from a commercial lipid mixture (Sigma) containing 63 μmol L-α-phosphatidyl choline, 18 μmol diacetylphosphate, and 9 μmol cholesterol. Lipids were resuspended in 5 ml methanol:chloroform (1:2) and placed in a 250-ml round-bottom flask, and the solvent was removed under vacuum. The lipid film was brought into suspension by adding 5 ml of a solution containing 100 mM KCl and 10 mM HEPES at pH 7.2 to a rotary evaporator flask along with 0.5 g of glass beads (150–200 μm diameter; Sigma) and rotating the flask continuously for 30 min. After standing for 1 h, the liposomes were decanted and stored under nitrogen at 4°C.

Indicator binding to liposomes

A 300-μl aliquot of liposome suspension (3.6 μmol of lipid) was mixed with 2 μl of 1 mM fura-2 or FFP18 stock and incubated for 4 h at room temperature. Liposomes were then pelleted by centrifugation overnight at 175,000 × g, and the supernatant was removed and diluted to 3 ml in 100 mM KCl and 10 mM HEPES, pH 7.2 (buffer A). The pellet was resuspended in 200 μl of buffer A and pelleted again at 175,000 × g for 4 h. The washed pellets were suspended in 3 ml of buffer A. Fluorescence intensities of supernatants and washed pellets were measured at 362 nm excitation and 510 nm emission.

RESULTS

Organic synthesis

The new indicators PE3 and FFP18 are analogs of the fluorescent calcium indicator fura-2, which is in turn a derivative of BAPTA (Fig. 1 *A*; Grynkiewicz et al., 1985; Tsien, 1980). In fura-2 one of the aromatic BAPTA rings (ring A, Fig. 1 *A*) has been modified to give a fluorescent benzofuran oxazole carboxylic acid. The hypothesis that zwitterionic indicators would be better retained in the cytosol was initially tested by making derivatives of the fura-2 oxazole carboxylic acid. One example is PE1, which is shown in Fig. 1 *B*. Although PE1 leaked out of cells much more slowly than fura-2 (Poenie and Chen, 1993), preliminary studies indicated that PE1 was not as bright as fura-2 (Bill Busa, unpublished results). Because the results obtained with PE1 were promising, new efforts were aimed at making a more versatile zwitterionic BAPTA backbone, which avoided modifications to the fluorophore. The first of these attempts is represented by PE2. Here, in an effort

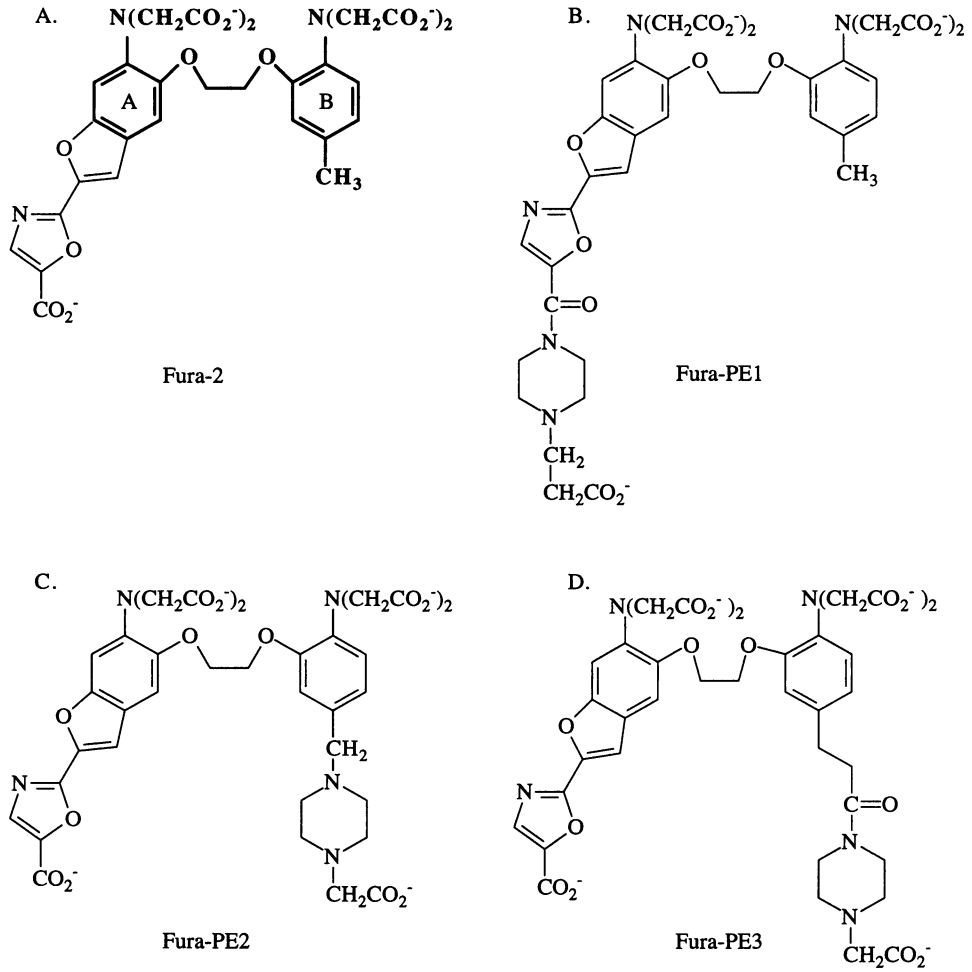

FIGURE 1 A comparison of structures of fura-2, and several versions of the zwitterionic calcium indicators: fura-PE1, fura-PE2, and fura-PE3. (*A*) The structure of fura-2 is shown and the features common to BAPTA are highlighted in bold lettering. The two aromatic rings are designated A and B for later reference. (*B*) Fura-PE1 is a zwitterionic analog of fura-2 in which a piperazinoacetic acid group is linked to the oxazole carboxylic acid. This indicator was retained in the cytosol but was dimmer than fura-2. (*C*) Fura-PE2 is another zwitterionic analog of fura-2 in which the number of additional carbons was minimized by linking piperazineoacetic acid to the benzylic carbon on ring B. In this case both piperazine amino groups are free to ionize. Unfortunately, PE2 was too pH sensitive. (*D*) Fura-PE3 is similar to fura-PE2, but one of the piperazine nitrogens is incorporated into an amide bond and there are more carbon atoms separating the ionizable amine from the BAPTA B ring.

to minimize hydrophobicity, piperazine was linked to the benzylic methyl group on ring B (Fig. 1 *C*). Unfortunately, the ionizable piperazine nitrogen was not sufficiently insulated from the BAPTA ring, resulting in an indicator that was too pH sensitive. Better insulation was obtained when the piperazine and BAPTA rings were separated by more carbon atoms, as shown for PE3 (Fig. 1 *D*). This was achieved by substituting 3-hydroxy-4-nitrobenzaldehyde (Fig. 2, II) for the 2-nitro-5-methylphenol used in the original synthesis of fura-2. A Wittig reaction between the aldehyde of compound III and the phosphorane of *t*-butylbromoacetate gave an unsaturated α,β linkage (V), which was then reduced by catalytic hydrogenation, along with the two aromatic nitro groups, to give compound VI. The advantage of using *t*-butylbromoacetate is seen later in the synthesis, when it becomes necessary to selectively deprotect this carboxyl group while leaving the remaining carboxylate esters intact. Between compound VI and compound X (FF6) the synthetic steps are virtually identical to those used for the synthesis of fura-2.

FF6 is a key intermediate containing an aliphatic 3 carbon linker arm terminated in a protected carboxyl group. The *t*-butyl ester can be selectively removed with TFA to give XI, which frees the carboxyl group for further substitution. The two FF6 derivatives synthesized in this study were PE3 and FFP18. With PE3 we sought to incorporate an ionizable amino group that could survive acetoxymethyl esterification without quaternization. Several different amine derivatives were explored. We found that methyl-2-(1-piperazino)acetate (XII) could be easily linked to the indicator through an amide linkage. The remaining tertiary amine was resistant to quaternization during subsequent synthesis of the acetoxymethyl ester. The FFP18 is similar to PE3 but incorporates a different piperazine adduct, 1-dodecylpiperazine. Here a 12-carbon tail linked to one of the piperazine

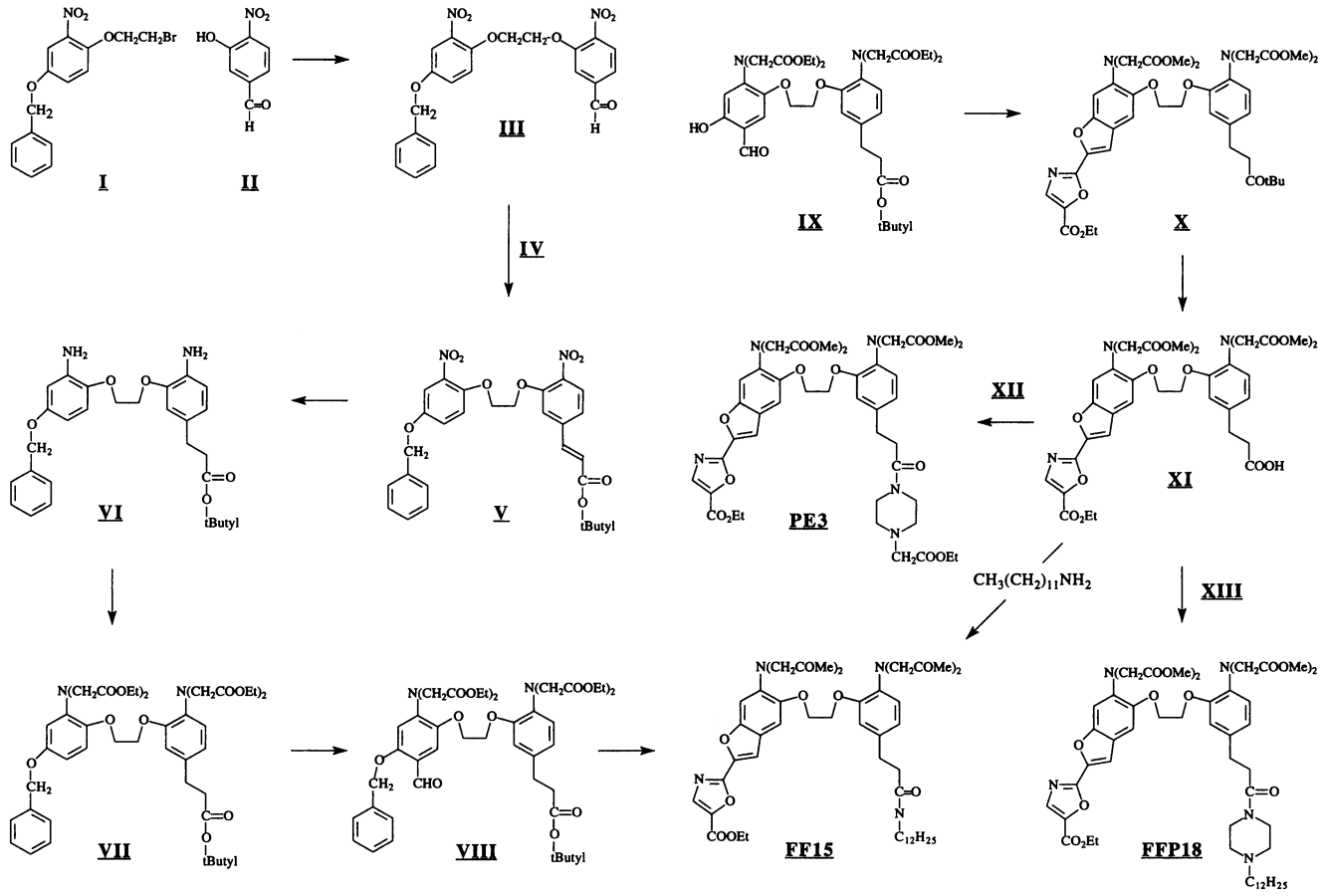

FIGURE 2 Schematic of the organic synthesis. The synthetic pathway leading to PE3, FF15, and FFP18 is depicted with intermediates labeled with Roman numerals. (*A*) Intermediates I–VIII. (*B*) The continuation from IX to PE3, FF15 and FFP18.

amino groups gives the indicator an affinity for lipid membranes.

The properties of PE3

The goal for PE3 was a zwitterionic calcium indicator that retained the spectral properties, ion selectivity, pH insensitivity, and noninvasive loading capabilities of fura-2. By avoiding modifications to the chromophore, this aim was largely achieved. Comparison of the absorbance and fluorescence spectra of fura-2 PE3 shows that the two compounds are nearly identical in their spectral properties (Table 1).

The calcium and magnesium dissociation constants for PE3 at 20°C and 37°C were determined from incremental titration of the indicator with each ion. Sets of fluorescence excitation spectra obtained from titration of PE3 with Ca^{2+} are shown in Figs. 3 and 4, respectively. A computer program was then used to generate Hill plots and to determine the calcium K_d from the titration data. The results, given in Table 1, show that in comparison to fura-2, PE3 has a slightly lower affinity for calcium and a slightly higher affinity for magnesium.

An important concern in the design of PE3 was its pH sensitivity. Changes in electron withdrawing effects of the protonated and unprotonated piperazine amino group, if communicated to the aromatic ring, would have an impact on the affinity for metal ions. This creates the potential for a complex mixture of indicators in solution where protonated and unprotonated forms would have different calcium dissociation constants. To determine the pH sensitivity of PE3, calcium K_d values were determined at different pH values. The results show that between pH 6.9 and 7.3, the calcium K_d of PE3 changes from 269 nM to 204 nM (Table 2). This is similar to the results obtained with fura-2, whose calcium K_d changed from 216 nM to 161 nM over the same pH range. Thus the pH sensitivity of PE3 is similar to that of fura-2 and not primarily a function of the piperazine moiety.

One of the advantages of the tetracarboxylate family of calcium indicators is their ability to load into cells as membrane-permeant AM ester derivatives. When cells are incubated with the AM ester derivative, the indicator enters the cytoplasm, where cytoplasmic esterases remove the protecting ester groups, trapping the indicator in the cytosol. To determine if PE3 could load in a similar manner, the

TABLE 1 Physical properties of PE3 and FFP18

Dye	Peak absorption wavelength (nm)		Peak emission wavelength (nm)		Calcium K_d (nM)		Magnesium K_d (mM)		Fluorescence quantum efficiency	
	Ca bound	Free anion	Ca bound	Free anion	20°C	37°C	20°C	37°C	Ca bound	Free anion
fura-PE3	335	364	495	508	204*	290‡	4.3	4.0	0.43	0.27
FFP18	335	364	490	502	331* (510)¶	415§ (400)‖	6.8	3.3	0.46	0.25
fura-2	336	364	505	510	161*	224**	9.8**	5.6**	0.49**	0.23**

*100 mM KCl, 10 mM MOPS, pH 7.3, 20°C. Apparent K_d of CaEGTA was 95.4 nM.

‡130 mM KCl, 20 mM NaCl, 1 mM free $MgCl_2$, 10 mM 4-morpholinepropanesulfonic acid (MOPS), pH 7.05, 37°C. Apparent K_d of CaEGTA used was 214 nM with an apparent K_d for MgEGTA of 8.96 mM.

§130 mM KCl, 20 mM NaCl, 1 mM free $MgCl_2$, 10 mM MOPS, pH 6.9, 37°C. Apparent K_d of CaEGTA used was 423 nM with an apparent K_d for MgEGTA of 14.7 mM.

¶FFP18 was adsorbed to liposomes, which were then pelleted and resuspended in 100 mM KCl, 10 mM HEPES, pH 7.2, and titrated at 20°C.

‖FFP18 was adsorbed to liposomes, which were then pelleted and resuspended in 100 mM KCl, 10 mM HEPES, pH 7.2, and titrated at 37°C.

**Data from Grynkiewicz et al. (1985).

PE3/AM ester was synthesized as described in Materials and Methods and tested with 322 T-lymphoma cells.

To evaluate dye loading and hydrolysis, 322 T lymphoma cells were loaded with either 1 μM fura-2/AM for 30 min or 2 μM PE3/AM for 1 h at 37°C. After loading, cells were pelleted by centrifugation, resuspended in HBSS containing 1.2 mM Ca^{2+}, and incubated at 37°C for an additional 10 min. Fluorescence at 340 nm and 380 nm excitation (510 nm emission) was recorded after lysis with 100 μM digitonin and subsequently, after the addition of 10 mM K_2H_2EGTA and 20 mM Tris base. R_{min} and R_{max} values were also obtained from samples of the fura-2 or PE3 salts. A comparison of R_{min} and R_{max} values obtained from loaded cells after lysis and from the pure salts is presented in Table 3. The results show that both the fura-2/AM and PE3/AM ester loaded cells give R_{max} values that are about 90% of those obtained from the indicator salts. Although these

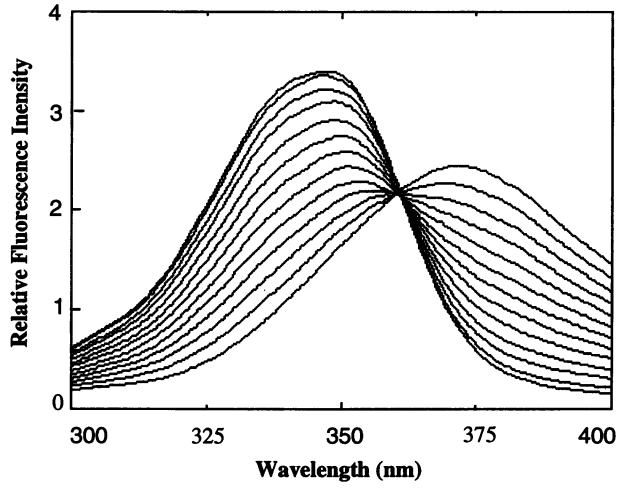

FIGURE 3 Fluorescence excitation spectra of PE3 as a function of $[Ca^{2+}]$. Spectra were recorded using a Photon Technology Alphascan fluorometer with the excitation bandwidth set to 4 nm and the emission monochromator set to 510 nm with a 5-nm band width. The titration began with 3 ml of a solution containing 100 mM KCl, 10 mM MOPS, 10 mM EGTA, and 200 nM fura-PE3 at pH 7.2 with the temperature maintained at 20°C by a circulating water bath. After an excitation spectrum was recorded, $[Ca^{2+}]$ was incrementally increased by iteratively discarding a volume of solution and adding an equivalent volume of solution containing 100 mM KCl, 10 mM MOPS, 10 mM CaEGTA, and 200 nM fura-PE3 at pH 7.2 as described previously (Grynkiewicz et al., 1985). Assuming an apparent dissociation constant of 151 nM for EGTA, this series of iterations gave free calcium concentrations of 17 nM, 38 nM, 65 nM, 101 nM, 151 nM, 227 nM, 363 nM, 604 nM, 1.38 μM, 4.38 μM, and 30 μM. For the last trace, $CaCl_2$ was added to a final concentration of 1 mM.

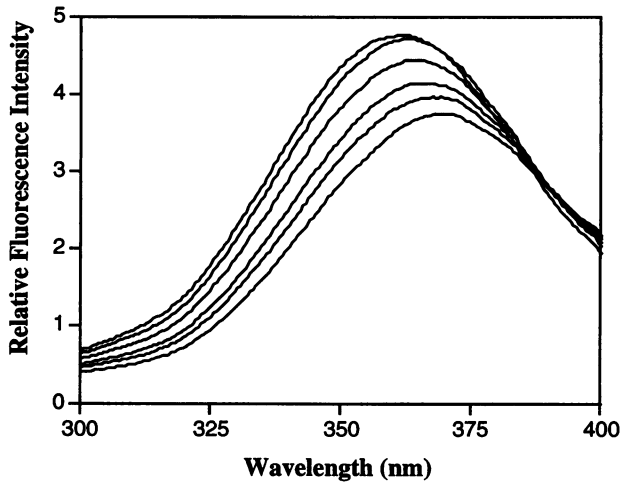

FIGURE 4 Fluorescence response of PE3 to Mg^{2+}. A fluorescence excitation spectrum was recorded from 2.5 ml solution containing 1 μM fura-PE3, 130 mM KCl, 20 mM NaCl, 1 mM EGTA, and 10 mM MOPS adjusted to pH 7.05 and maintained at 37°C by a circulating water bath. The slits on the excitation monochromator were set for a 4-nm bandwidth, and the emission monochromator was set to 490 nm with a 5-nm bandwidth. After the first spectrum was recorded, 25 μl of the solution was replaced with 25 μl of a solution containing 1 μM PE3, 111.2 mM $MgCl_2$, 12.2 mM EGTA, and 10 mM MOPS adjusted to pH 7.05. Assuming an apparent dissociation constant of 8.96 mM, this exchange gave 1 mM free Mg^{2+}. Successive exchanges of 25.25, 76.53, 131.6, 277.8, and 625 μl gave, respectively, 2.5 mM, 5 mM, 10 mM, 20 mM, and 40 mM free Mg^{2+}.

TABLE 2 Sensitivity of PE3, FFP18, and Fura-2 to pH

	pH 6.9	pH 7.3	ΔK_d
Fura2	216 ± 4	161 ± 2	55
PE3	269 ± 3	204 ± 4	65
FFP18	411 ± 5	331 ± 2	80

Titrations were carried out in 100 mM KCl, 10 mM MOPS at 20°C, and dissociation constants were determined assuming an apparent K_d for EGTA of 594 nM at pH 6.9 and 95.4 nM at pH 7.3.

results suggest that hydrolysis might not be complete, they also indicate that PE3 is no worse than fura-2.

The quality of dye loading was also analyzed by measuring the fluorescence response at 340 nm and 380 nm excitation while manipulating $[Ca^{2+}]_i$. An example of the results are shown in Fig. 5. In this experiment, 322 T lymphoma cells suspended at a concentration of 10^6 cells/ml were loaded with 2 μM PE3 or 1 μM fura-2/AM. The suspension was then treated with 40 μg/ml concanavalin A, which stimulates an increase in $[Ca^{2+}]_i$ by stimulating the T cell receptor. Subsequently, 2 μM ionomycin was added, resulting in an even larger fluorescence response. Afterward, 100 μM digitonin was added to lyse the cells and obtain the fluorescence response at saturating calcium. Finally, 10 mM EGTA and 20 mM Tris base were added to obtain the fluorescence signal for the low $[Ca^{2+}]$ end point. Experiments such as those shown in Fig. 5 were carried out several times and averaged for both fura-2 and PE3. The data for these experiments are summarized in Table 3.

To compare the tendencies of fura-2 or PE3 to leak out of cells, suspensions of cells loaded with fura-2 or PE3 were treated with Ni^{2+} immediately after loading or after a 1-h incubation. Nickel is similar to manganese in its ability to quench the fluorescence of fura-2, but manganese is not as effective with PE3. In these experiments, the difference in fluorescence intensity, measured at 362 nm, before and after adding $NiCl_2$, represents the fraction of the indicator that

TABLE 3 Comparison of fura2/AM and PE3/AM hydrolysis

	Fura-2	PE3
K^+ salt R_{max}	13.0	9.6
K^+ salt R_{min}	0.52	0.53
AM R_{max}	12.0	8.7
AM R_{min}	0.52	0.53
% theoretical	90	91
F380 EGTA*	2.8×10^4	2.9×10^4

Cells were loaded with either 1 μM fura-2/am for 30 min or 2 μM PE3/AM for 1 h, washed, and resuspended and incubated for 10 min in HBSS containing 1.2 mM calcium and 1% FBS. Fluorescence was recorded from the cell suspension at 510 nM emission and 340 nm or 380 nm excitation. To obtain R_{max} and R_{min} the 340 nm/380 nm fluorescence ratios were determined for loaded cells immediately after lysis with 100 μM digitonin (R_{max}) and then after the addition of 10 mM K_2H_2EGTA and 20 mM Tris base (R_{min}). Similar measurements were made for 1 μM solutions of fura-2 or PE3 potassium salt dissolved in HBSS.

*The fluorescence signal at 380 nm excitation obtained from a lysed suspension of fura-2/AM- or PE3/AM-loaded cells after addition of EGTA and Tris base.

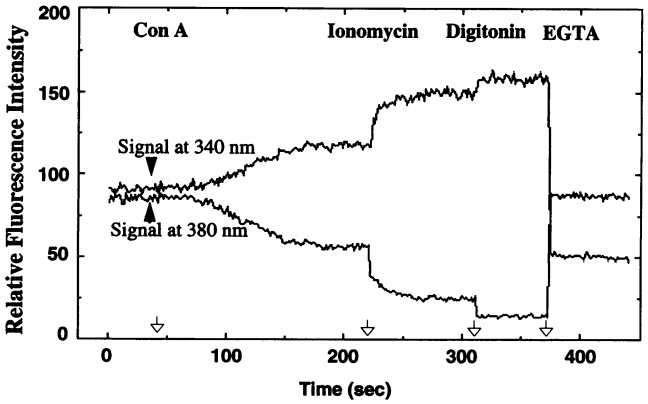

FIGURE 5 The responsiveness of PE3-loaded cells to changes in $[Ca^{2+}]_i$. For loading with PE3, 322 T-lymphoma cells were suspended at a concentration of 1×10^6/ml in RPMI containing 1% FBS, 2 μM PE3/AM and 10 mM HEPES adjusted to pH 7.0 and incubated at 37°C for 2 h. Afterward, cells were washed by gentle centrifugation and resuspended in HBSS containing 1% FBS and 10 mM HEPES, pH 7.2, containing 5×10^5 cells/ml. An aliquot of this loaded cell suspension was then placed in a cuvette maintained at 37°C by a circulating water bath. Fluorescence was excited alternatively at 340 nm and 380 nm, and the signal at each excitation wavelength was plotted against time. The baseline measurements were recorded for 50 s, and then cells were stimulated with 40 μg/ml Con A (*first arrow*), which activates T-cells by ligating the T-cell antigen receptor. After the response to Con A developed, 1 μM ionomycin was added (*second arrow*) to further elevate $[Ca^{2+}]_i$. Cells were then lysed with 100 μM digitonin, exposing the indicator to saturating levels of Ca^{2+} (*third arrow*). Subsequently, 10 mM EGTA and 20 mM Tris base were added to reduce free calcium levels to 10^{-9} M (*fourth arrow*).

has leaked into the extracellular medium. A comparison of the data obtained at time zero and at 1 h after loading shows that fura-2 leaks out of cells much more rapidly than PE3 (Fig. 6). Trypan blue exclusion tests, which were carried out for each measurement, always gave better than 95% viability, showing that the increase in extracellular indicator was not due to cell lysis.

The leakage of indicator out of the cells can complicate calcium measurements in several different ways. This is illustrated in Fig. 7, where 322 cells were loaded with fura-2 or PE3 and apparent $[Ca^{2+}]_i$ of unstimulated cells was monitored in the fluorometer over an extended period of time. In the case of fura-2-loaded cells, baseline $[Ca^{2+}]_i$ appears to drift upward rapidly, whereas over the same time period, PE3-loaded cells showed relatively little change. Trypan blue exclusion revealed more than 95% viability before and after the measurement. However, when 4 mM $NiCl_2$ was added to quench the fluorescence of extracellular dye, apparent calcium levels instantly return to initial resting levels. Excess $NiCl_2$ was added to ensure maximal quenching of the extracellular indicator. The reduction in apparent $[Ca^{2+}]_i$ after the addition of $NiCl_2$ shows that the drift in apparent $[Ca^{2+}]_i$ is really due to leakage of the indicator into the extracellular medium.

Although the results obtained above using suspensions of 322 cells demonstrate that PE3 leaks out of cells more slowly than fura-2, they do not directly address the issue of

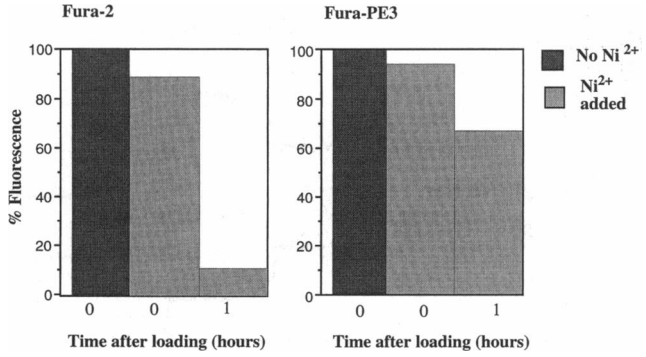

FIGURE 6 Rates of dye leakage from cells loaded with PE3 or fura-2. The 322 lymphoma cells were loaded with 2 μM fura-2/AM or 2 μM PE3/AM for 30 min or 1 h, respectively, in RPMI containing 1% FBS. In the case of fura-2 loading, pH of the medium was 7.2, whereas for PE3 loading the medium was adjusted to pH 6.8. After loading, the cells were gently pelleted and resuspended in HBSS containing 1% FBS and 10 mM HEPES adjusted to pH 7.2. An aliquot of loaded cells were placed in a cuvette and the fluorescence at 362 nm excitation (510 emission) is taken as the reference value (100% fluorescence). Subsequently, 2 mM Ni^{2+} was added to quench any indicator that was outside the cells, and this value is given as a percentage of the initial intensity. The remainder of the loaded cell suspension was incubated for 1 h at 37°C. A second aliquot was removed and placed in a cuvette together with 2 mM Ni^{2+} and the fluorescence was recorded. The difference in fluorescence of Ni^{2+}-treated cells between the zero and 1-h time points corresponds to the amount of indicator that leaked out of the cells into the extracellular medium.

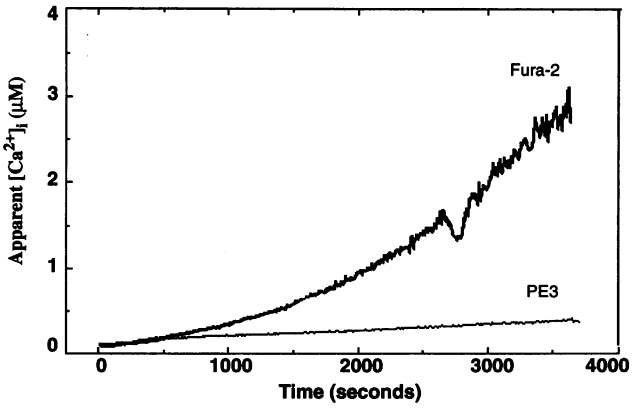

FIGURE 7 Baseline drift in apparent $[Ca^{2+}]_i$ of 322 cells loaded with PE3 or fura-2. Apparent baseline $[Ca^{2+}]_i$ levels were compared for 322 T-lymphoma cells loaded with either fura-2 or PE3. For loading, 1×10^6 cells/ml were incubated with either 2 μM fura-2/AM for 30 min (pH 7.2) or with 2 μM PE3/AM (pH 6.8) for 1 h. Afterward cells were washed by gentle centrifugation and resuspended at 1×10^6 cells/ml in HBSS containing 1% FBS and 10 mM HEPES adjusted to pH 7.2. Fluorescence measurements were obtained from 3 ml of cell suspension in a cuvette with excitation wavelengths alternating between 340 nm and 380 nm. The temperature was maintained at 37°C by a thermostated circulating water bath. Calcium concentration was calculated from the 340/385 nm fluorescence ratio as described previously and plotted. The figure shows apparent $[Ca^{2+}]_i$ over time for fura-2 (*darker trace*) and PE3 (*lighter trace*) loaded cells over time.

compartmentalization. Compartmentalization is more easily studied by using flattened adherent cells together with fluorescence imaging. Here the accumulation of dye into organelles is typically seen as a bright ring of fluorescence around the nucleus due to the accumulation of indicator into perinuclear organelles.

To compare compartmentalization and leakage of PE3 and fura-2 in adherent cells, we employed the BPV cell line. The BPV cells were used here because in previous studies using fura-2, these cells showed especially high rates of compartmentalization and leakage. Fig. 8 shows a series of fluorescence images of BPV cells loaded with either PE3 (Fig. 8, *A–F*) or fura-2 (Fig. 8, *G–L*) acquired at 362 nm excitation beginning immediately after cells were loaded and washed and extending over a period of 100 min. Whereas the cells loaded with PE3 do show a gradual decrease in fluorescence intensity over the 100-min interval, nearly all of the cytosolic fluorescence of the fura-2 loaded cells is gone by 20 min (see Fig. 8 *H*). In addition, cells loaded with PE3 appear uniformly fluorescent throughout the observation period. By contrast, 20 min after cells are loaded with fura-2, the residual fluorescence is largely confined to perinuclear organelles. These results suggest that PE3 resists both leakage and compartmentalization.

Properties of FFP18

The FF6 intermediate used in the synthesize of PE3 provided a flexible synthetic starting point for a number of different indicators. An alternative derivative is seen in the amphipathic calcium indicators FF15 and FFP18. These indicators contain a hydrophobic 12-carbon aliphatic tail. FF15 was the first structure synthesized and showed properties similar to those of fura-2 when in free solution. However, FF15 consistently failed to sense elevations in $[Ca^{2+}]_i$ after it was microinjected into cells (Alderton and Steinhardt, Harootunian and Tsien, personal communications). We hypothesized that when FF15 associated with membranes, the calcium-binding domain of the indicator was pulled into the lipid bilayer. Because the calcium-binding domain was sterically hindered by the lipid membrane, the indicator failed to report changes in calcium concentration. To avoid this problem, a piperazine moiety was added between the BAPTA ring and the hydrophobic tail to give FFP18. The positively charged piperazine nitrogen could presumably aid in binding to membrane phospholipids while preventing penetration of the calcium-binding portion of the indicator into the bilayer. Tests showed that when FFP18 was microinjected into cells, elevation of $[Ca^{2+}]_i$ was readily detected (Etter et al., 1994; Harootunian and Tsien, personal communication).

The spectral and binding properties of FFP18 were analyzed in a manner similar to that of PE3. Spectral data which show that FFP18 is similar to PE3 in its absorbance and fluorescence properties are summarized in Table 1. It should be noted, however, that emission scans obtained of FFP18 as $[Ca^{2+}]$ or pH was varied showed small variations in peak emission wavelengths but with no sharp isoemission point.

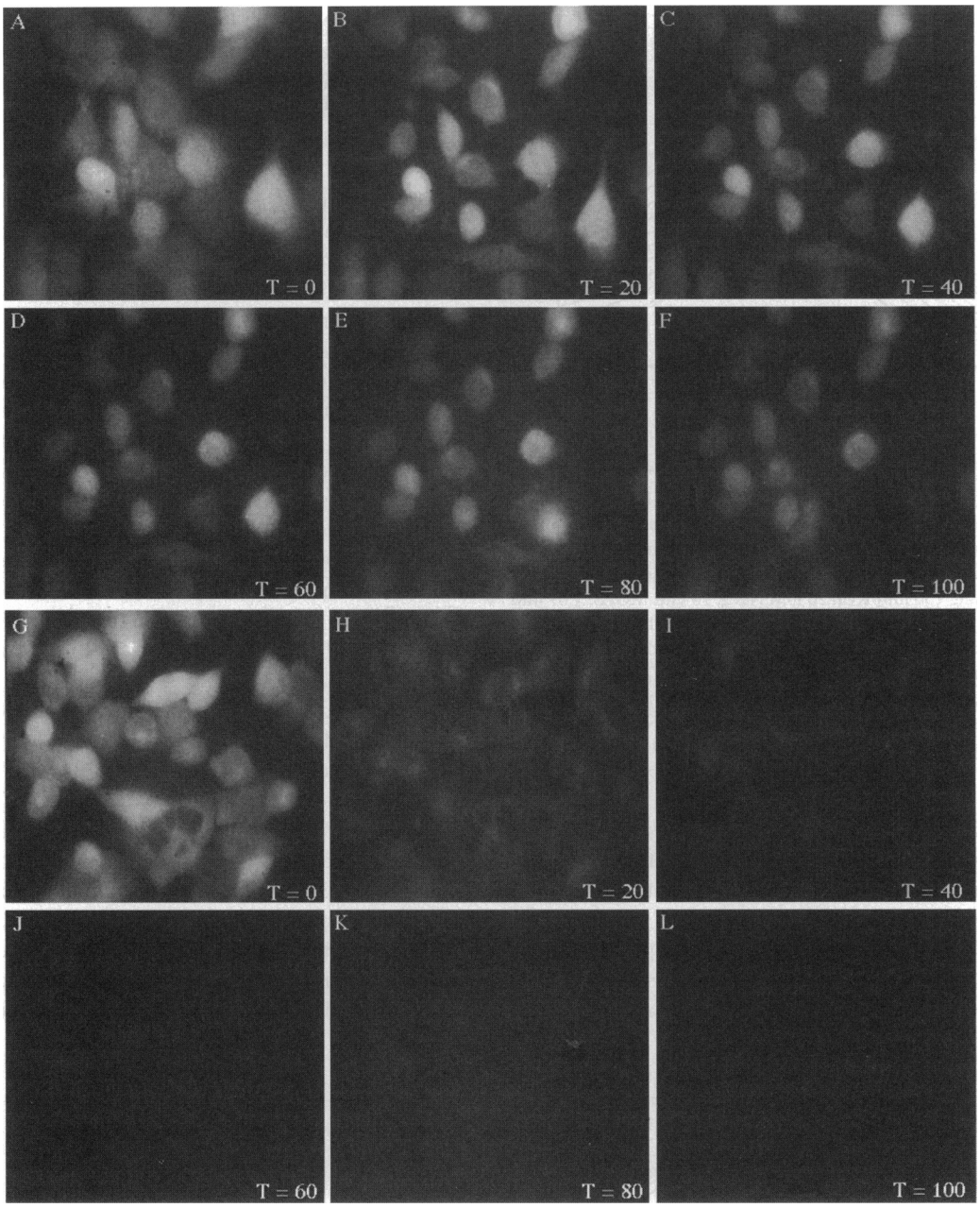

FIGURE 8 A visual comparison of fura-2 and PE3 leakage and compartmentalization in BPV cells. BPV cells, adhered to coverslips, were loaded with PE3/AM or fura-2/AM as described in Materials and Methods. Cells were mounted in a Sykes-Moore chamber and placed on a water-jacketed holder of a Zeiss IM-35 microscope. The temperature was maintained at 37°C in the sample chamber by a thermostatically controlled circulating water bath. Images were acquired with a Hammamasu SIT camera and a Photon Technology Image Master illumination and acquisition system. Images of the same microscope field were recorded at 360 nm excitation at 20-min intervals beginning immediately after cells were washed. Camera gain and intensifier voltages were set based on the brightness of cells at the first time point and maintained constant thereafter. Between the acquisition of images, excitation light was blocked by a shutter. (*A–F*) The upper series of photographs shows the patter of fluorescence change for PE3 loaded BPV cells. (*G–L*) The lower series of photographs shows the corresponding changes in fura-2-loaded BPV cells.

These problems were minimized when 490 nm was used as the emission wavelength.

Fig. 9 and 10 show typical sets of fluorescent spectra obtained during the titration of FFP18 with Ca^{2+} and Mg^{2+}, respectively. Analysis of these sets of spectra using Hill plots indicate that FFP18 has a substantially weaker affinity for calcium than either fura-2 or PE3 but retains good selectivity for calcium over magnesium (Table 1).

The pH sensitivity of FFP18 was evaluated by determining the calcium K_d at pH values of 6.9 and 7.3, as described previously for PE3 and fura-2 (Table 2). The results show that FFP18 is slightly more pH sensitive than PE3 or fura-2. However, the fluorescence of FFP18 also exhibited small changes in intensity due to pH alone. For example, there is a reversible 3–5% loss in intensity at 380 nm when the pH is raised from 7.0 to 8.5, with the most prominent transition occurring at pH

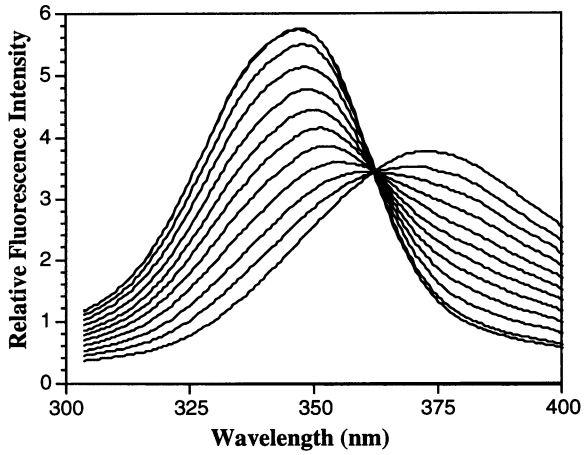

FIGURE 9 Excitation spectra for 333 nM FFP18 at 37°C in buffers with 1 mM free Mg^{2+} and free Ca^{2+} values ranging from <1 nM to >1 μM. Spectra were recorded with a Photon Technology Alphascan fluorometer with the excitation bandwidth set to 5 nm and the emission wavelength set to 485 nm with a 4-nm bandwidth. Titrations were carried out in 3 ml of a solution containing 130 mM KCl, 20 mM NaCl, 10 mM MOPS, 1.07 mM EGTA, 1.07 mM $MgCl_2$, and 333 nM fura-FFP18 with the pH adjusted to 6.9. After the initial excitation spectrum was recorded, calcium levels were adjusted incrementally by the addition of 0.5 M CaEGTA to 47 nM, 106 nM, 184 nM, 282 nM, 423 nM, 635 nM, 987 nM, 1.7 μM, and 30 μM, assuming an apparent dissociation constant of 423 nM. For the final trace, $CaCl_2$ was added to give 2 mM [Ca^{2+}].

7.5. This may indicate the formation of an intramolecular complex when the piperazine amine is protonated.

The incorporation of a hydrophobic tail into FFP18 was intended to generate a "membrane-anchored" calcium indicator. The choice of chain length for the lipophilic tail was based on preliminary data showing that a 12-carbon tail was a good compromise between hydrophobicity and water solubility. To determine the avidity of FFP18 for phospholipids, FFP18 was incubated with a suspension of liposomes as described in Materials and Methods. The results show that 87% of FFP18 remained associated with the liposome pellet. For fura-2, less than 1% of the dye pelleted with liposomes.

The binding of FFP18 to phospholipid bilayers could potentially change both spectral and ion-binding characteristics of the indicator from those seen in free solution. Thus it was essential to determine both spectral characteristics and the calcium K_d for liposome-bound FFP18. To evaluate these properties, liposome pellets containing bound FFP18 were prepared as described above. The liposome pellets were then resuspended in buffer and titrated with calcium at 20°C and at 37°C. Fig. 11 shows a set of fluorescence excitation spectra obtained from the titration of FFP18 bound to liposomes at 20°C. The fluorescence spectra of liposome-bound FFP18 show differences from that of FFP18 in aqueous solution. Overall, the dynamic range of FFP18 is reduced when bound to liposomes. In addition, the calcium K_d for FFP18 bound to liposomes at 20°C is 510 nM, which is significantly higher than that for FFP18 free in solution (see Table 1).

Another important characteristic of FFP18 concerns its solubility and tendency to aggregate. The hydrophobic tail on FFP18 should reduce the solubility of FFP18 as compared to fura-2 or PE3, and the formation of aggregates or precipitates would also likely alter the fluorescence spectrum. We evaluated these properties, monitoring the fluorescence and solubility properties of FFP18 over a range of dye concentrations. Solutions were prepared containing 1, 10, 50, or 100 μM FFP18 K^+ salt in a buffer containing 100 mM KCl and 10 mM HEPES (pH 7.0). The results show that the 1 and 10 μM concentrations were identical in their

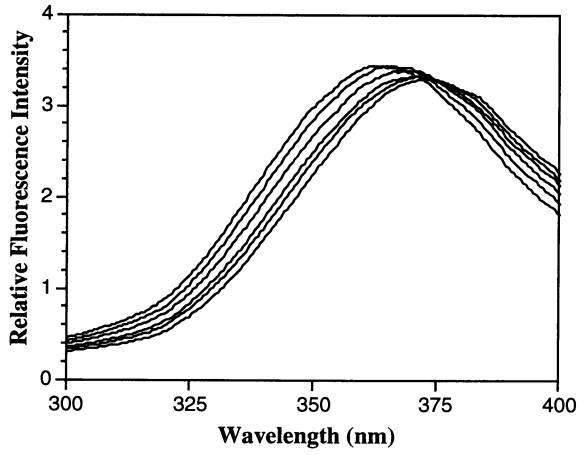

FIGURE 10 Fluorescence response of FFP18 to Mg^{2+}. A fluorescence excitation spectrum was recorded from 2.5 ml solution containing 1 μM FFP18, 130 mM KCl, 20 mM NaCl, 1 mM EGTA, and 10 mM MOPS adjusted to pH 7.05 and maintained at 37°C by a circulating water bath. The slits on the excitation monochromator were set for a 4-nm bandwidth and the emission monochromator was set to 485 nm with a 5-nm bandwidth. Titration with Mg^{2+} was carried out as described for PE3.

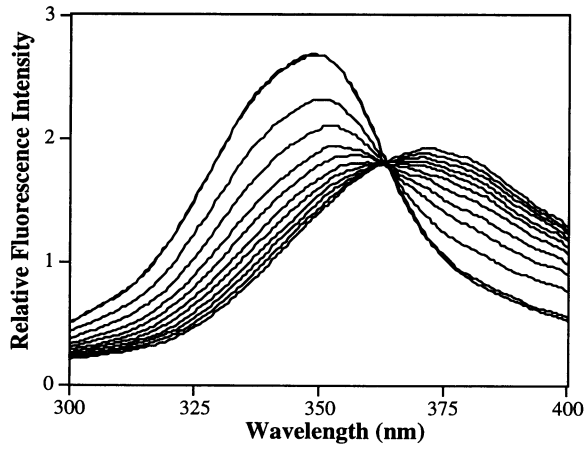

FIGURE 11 Titration of FFP18 bound to liposomes. Washed FFP18-bound liposomes were prepared as described in Materials and Methods and suspended in 3 ml of solution containing 100 mM KCl, 10 mM K_2H_2EGTA, and 10 mM HEPES adjusted to pH 7.2. The indicator was then titrated at 20°C as described for PE3. Excitation spectra were recorded at a bandwidth of 4 nm for the excitation monochromator and at 485 nm emission with a bandwidth of 5 nm for the emission monochromator.

fluorescence and calcium-binding properties but significant differences were seen in the 50 and 100 μM samples. Samples containing 50 μM or more FFP18 exhibited some turbidity and did not respond to changes in $[Ca^{2+}]$. The fluorescence excitation maxima were also shifted toward longer wavelengths. These results suggest that FFP18 aggregates in aqueous solution at concentrations of 50 μM or above. However, the nature of these aggregates was not characterized. In practice, solutions containing 30 μM FFP18 have been used to load cells by microinjection. At these concentrations, FFP18 does not harm cells and cells are bright enough for imaging experiments (Elaine Etter and Fred Fay, personal communications).

DISCUSSION

The new calcium indicators described in this report provide important new advantages and capabilities. Dye leakage and compartmentalization complicate many aspects of calcium studies, including the determination of true resting calcium levels in cuvette-based measurements, interpretation of apparent calcium gradients in imaging studies, and the measurement of calcium over any significant period of time. In cases where leak rates are especially high, it may even be impossible to obtain good loading. With PE3, many of these problems are far less severe, so that cells can remain uniformly loaded and responsive for hours.

Despite its benefits, PE3 is still not the ideal cytosolic indicator. Leakage and compartmentalization are dramatically reduced but not eliminated. Although the PE3/AM ester can be used for loading the indicator into cells, it has a greater tendency to crystallize or precipitate than is seen with fura-2. This tends to reduce the efficiency of loading or, at high AM ester concentrations, to give cells with many attached dye particles. Attempts to optimize loading have shown that low concentrations (1–2 μM) of PE3/AM incubated with cells for 1–2 h at slightly acidic pH (6.7) have given the best results with T cell lines. For loading adherent cells, higher AM ester concentrations are needed. To overcome the problem of particulates, we have found that agitation of cells at 37°C gives good results. The use of pluronic F127 also reduces particulates and helps to load more indicator into the cell. Surprisingly, one expected problem appears to be insignificant. Many hydrophobic amines tend to partition into acidic intracellular compartments, and the PE3/AM could act similarly. If this were a problem, we would have expected PE3 to accumulate into lysosomes. In practice, the initial distribution of PE3 in freshly loaded cells is far more uniform than is seen with fura-2, and this diffuse distribution is maintained over time.

PE3 represents an improved fluorescent indicator for $[Ca^{2+}]_i$, but it is becoming clear that other types of calcium indicators are needed. There is increasing evidence that fura-2 can miss Ca^{2+} transients that are very fast or highly localized (Augustine and Neher, 1992; Kao et al., 1990; Klein et al., 1988). This potential problem was one of the motivations for developing a calcium indicator that could be targeted to membranes. There are numerous mathematical modeling studies that show when calcium enters the cell through channels in the plasma membrane, $[Ca^{2+}]_i$ near the site of calcium entry should be quite large (Sala and Hernandez-Cruz, 1990; Simon and Llinas, 1985; Fogelson and Zucker, 1985). Unfortunately, there is little direct experimental support for these models. However, the problem may lie in the calcium indicator rather than the model.

Recent studies comparing calcium signals reported by fura-2 or FFP18 under the same experimental conditions show dramatic differences in magnitude and kinetics. In one set of experiments where responses of fura-2 and FFP18 were compared in electrically stimulated smooth muscle cells, fura-2 showed a calcium rise that peaked at 150 ms, whereas calcium measured by FFP18 peaked before 12 ms (Etter et al., 1994b; Etter et al., submitted for publication). In addition, even though FFP18 has a weaker affinity for calcium than does fura-2, calcium peaks measured with FFP18 were often truncated, suggesting that the indicator may saturate during the transient. If so, peak calcium levels near membranes must rise to far higher levels than in the cytosol. To accurately track these high Ca^{2+} levels, analogs of FFP18 with lower calcium affinity are needed and their development is currently under way. Low-affinity near-membrane calcium indicators should also be correspondingly less sensitive to the much smaller changes in cytosolic $[Ca^{2+}]_i$. In addition, efforts are under way to obtain more selective targeting to the plasma membrane. It is hoped that these changes will yield indicators that selectively sense changes in Ca^{2+} due to the opening of calcium channels.

Preliminary results from studies using FFP18 are promising, but the spectral anomalies associated with FFP18 aggregation, its sensitivity to its environment, and its increased hydrophobicity suggest that this indicator will be more difficult to use than fura-2. Attempts to load FFP18 into cells as an acetoxymethyl ester have revealed that only about 50% of the ester is hydrolyzed and that therefore this is not a useful loading procedure. The marked differences in K_d seen for FFP18 in free solution and that bound to anionic liposomes shows how sensitive the indicator is to its environment and underscores the need for users to properly characterize the properties of the indicator in their own experimental systems. Yet despite these difficulties, efforts to use FFP18 as an intracellular calcium indicator have been successful. These studies, using FFP18 microinjected into cells, have confirmed the existence of large calcium transients near membranes that are not accurately tracked by fura-2 (Etter et al., in preparation).

Whereas FFP18 is targeted to membranes, there may be other microdomains within the cell cytoplasm where localized changes in Ca^{2+} are important but are largely missed by fura-2. To answer these questions it will be necessary to develop new indicators targeted to different regions within the cell. The flexibility of the FF6 structure should open the door to these new kinds of indicators. Conceivably, variants of XI could be linked to peptides or proteins to give indi-

cators targeted to almost any intracellular environment. For example, indicators linked to tubulin or actin could make it possible to monitor the impact of calcium on filament structure and function by visualizing both at the same time.

The ability to target fluorescent calcium indicators to specific intracellular environments offers exciting prospects for a new understanding of calcium signaling in cells, but it also adds a new level of complexity to the use of the indicators. It is well known that fluorophores are sensitive to their environment, and indicators like FFP18 are no exception. Titrations of FFP18 in free solution and FFP18 bound to liposomes, although similar to fura-2, show significant differences in their excitation and emission spectra. Given that it is not possible to determine the properties of the indicator for every possible environment, it will be critical for the user to analyze the spectral characteristics of the indicator under the actual experimental conditions rather than simply extrapolating from its properties in free solution. Fortunately, modern instruments make it possible to analyze the spectral behavior of fluorescent indicators from individual cells on the microscope stage.

This work was supported by grants GM40605 from the NIH and DCB 8858186 and DIR 9022325 from the NSF. During the course of this work Charles Vorndran received support under an NIH training grant number T32GM08368.

REFERENCES

Almers, W., and E. Neher. 1985. The Ca^{2+} signal from fura-2 loaded mast cells depends strongly on the method of loading. *FEBS Lett.* 192:13–18.

Augustine, G., and E. Neher. 1992. Calcium requirements for secretion in bovine chromaffin cells. *J. Physiol.* 450:247–271.

Di Virgilio, F., T. Steinburg, and S. Silverstein. 1990. Inhibition of Fura-2 sequestration and secretion with organic anion transport blockers. *Cell Calcium.* 11:57–62.

Di Virgilio, F., T. H. Steinberg, J. A. Swanson and S. C. Silverstein. 1988. Fura-2 secretion and sequestration in macrophages. A blocker of organic anion transport reveals that these processes occur via a membrane transport system for organic anions. *J. Immunol.* 140:915–920.

Etter, E. F., M. A. Kuhn, and F. S. Fay. 1994. Detection of changes in near membrane Ca^{2+} using a novel membrane associated Ca^{2+} indicator. *J. Biol. Chem.* 269:10141–10149.

Etter, E., M. Poenie, A. Minta, and F. S. Fay. 1994b. Monitoring near membrane changes in $[Ca^{2+}]_i$ in smooth muscle cells. *Biophys. J.* 66:A151.

Fogelson, A. L., and R. S. Zucker, 1985. Presynaptic calcium diffusion from various arrays of single channels. *Biophys. J.* 48:1003–1017.

Goligorsky, M., D. Loftus, and E. Elson. 1986. Alpha1-adrenergic stimulation and cytoplasmic free calcium concentration in cultures renal proximal tubular cells: evidence for compartmentalization of quin-2 and fura-2. *J. Cell Physiol.* 128:466–474.

Grynkiewicz, G., M. Poenie, and R. Tsien. 1985. A new generation of fluorescence Ca^{2+} indicators with greatly improved fluorescence properties. *J. Biol. Chem.* 260:3440–3450.

Hernandez-Cruz, A., F. Sala, and P. Adams. 1990. Subcellular calcium transients visualized by confocal microscopy in a voltage-clamped vertebrate neuron. *Science.* 247:858–862.

Hollingsworth, S., and S. Baylor. 1987. Fura-2 signals from intact frog skeletal muscle fibers. *Biophys. J.* 51:549a.

Kao, J., J. Alderton, R. Tsien, and R. Steinhardt. 1990. Active involvement of calcium in mitotic progression of Swiss 3T3 fibroblasts. *J. Cell Biol.* 111:183–196.

Klein, M., B. Simon, G. Szucs, and M. Schneider. 1988. Simultaneous recording of calcium transients in skeletal muscle using high- and low-affinity calcium indicators. *Biophys. J.* 53:971–988.

Llinas, R., M. Sugimori, and R. B. Silver. 1992. Microdomains of high calcium concentration in a presynaptic terminal. *Science.* 256:677–679.

Malgaroli, A., D. Milani, J. Meldolesi, and T. Pozzan. 1987. Fura-2 measurement of cytosolic free Ca^{2+} in monolayers and suspensions of various types of animal cells. *J. Cell Biol.* 105:2145–2155.

Moisescu, D., and H. Pusch. 1975. A pH metric method for the determination of the relative concentration of calcium to EGTA. *Pfleugers Arch.* 355:R122.

New, R. R. C., ed. 1990. Liposomes: A Practical Approach. IRL Press, New York.

Poenie, M. 1990. Alteration of intracellular fura-2 fluorescence by viscosity: a simple correction. *Cell Calcium.* 11:58–91.

Poenie, M., J. Alderton, R. Steinhardt, and R. Tsien. 1986. Calcium rises abruptly and briefly throughout the cell at the onset of anaphase. *Science.* 233:886–889.

Poenie, M., and C. S. Chen. 1993. New fluorescent probes for cell biology. *In* Optical Microscopy: Emerging Methods and Applications. B. Herman and L. Lemaster, editors. Academic Press, New York. 1–25.

Rasmussen, C. D., and A. R. Means. 1987. Calmodulin is involved in regulation of cell proliferation. *EMBO J.* 6:3961–3968.

Richie, E. R., B. McEntire, J. Phillips, and J. P. Allison. 1988. Altered expression of lymphocyte differentiation antigens on phorbol ester-activated CD4+8+ T cells. *J. Immunol.* 140:4115–4122.

Rizzuto, R., M. Brini, M. Murgia, and T. Pozzan. 1993. Microdomains with high Ca^{2+} close to IP3-sensitive channels that are sensed by neighboring mitochondria. *Science.* 262:744–747.

Sala, F., and A. Hernandez-Cruz. 1990. Calcium diffusion modeling in a spherical neuron. *Biophys. J.* 57:313–324.

Scanlon, M., D. Williams, and F. Fay. 1987. A Ca^{2+}-insensitive form of Fura-2 associated with polymorphonuclear leukocytes. *J. Biol. Chem.* 262:6308–6312.

Simon, S. M., and R. R. Llinas. 1985. Compartmentalization of the submembrane calcium activity during calcium influx and its significance in transmitter release. *Biophys. J.* 48:485–498.

Speksnijder, J. E., A. L. Miller, M. H. Weisenseel, T.-H. Chen, and L. F. Jaffe. 1989. Calcium buffer injections block fucoid egg development by facilitating calcium diffusion. *Proc. Natl. Acad. Sci. USA.* 86: 6607–6611.

Steinberg, S., J. Bilezikian, and Q. Al-Awaqati. 1987. Fura-2 fluorescence is localized to mitochondria in endothelial cells. *Am. J. Physiol.* 253: C744–C747.

Tsien, R. 1980. New calcium indicators and buffers with high selectivity against magnesium and protons: design, synthesis, and properties of prototype structures. *Biochemistry.* 19:2396–2404.

Tsien, R., and T. Pozzan. 1989. Measurement of cytosolic free calcium with Quin2. *Methods Enzymol.* 172:230–263.

Tsien, R. Y., and T. J. Rink. 1980. Neutral carrier ion-selective microelectrodes for measurement of intracellular free calcium. *Biochim. Biophys. Acta.* 599:623–638.

Tsien, R. Y., T. J. Rink, and M. Poenie. 1985. Measurement of cytosolic free Ca^{2+} in individual small cells using fluorescence microscopy with dual excitation wavelengths. *Cell Calcium.* 6:145–157.